

Quasi-Coherent Molecular Vibrations with Energies above the Dissociation Threshold in the Ground Electronic State

J. Manz, M. Oppel,* and G. K. Paramonov†

*Institut für Physikalische und Theoretische Chemie, Freie Universität Berlin,
WE 3, Takustrasse 3, D-14195 Berlin, Germany*

Received: November 14, 1997; In Final Form: January 30, 1998

Selective infrared laser pulses in the femtosecond (fs) time domain may be used to prepare quasi-coherent molecular vibrations in the dissociative continuum of the ground electronic state. These vibrations may be monitored by femtosecond IR+UV pump–probe spectroscopy. The new phenomenon is discovered by means of molecular wave-packet simulations for a two-dimensional model based on ab initio potential-energy surfaces and dipole functions for HONO₂.

1. Introduction

The purpose of this paper is to present a new type of molecular vibration that may be prepared and monitored by IR and UV laser pulses in the femtosecond time domain: quasi-coherent vibrations in the ground electronic state but with energies well above the dissociation threshold and even above any potential barriers. (The word “quasi-coherent” indicates certain deviations from perfect coherent vibrations, which exist only in ideal model systems, e.g., harmonic oscillators.¹) More specifically, we show that molecules may absorb vibrational energy in both dissociative and nondissociative “spectator” bonds such that the dissociative bond oscillates in a quasi-periodic fashion and with rather long lifetimes ($\gg 10$ ps), that is, without any abrupt cleavage, which is blocked, even though the total amount of vibrational energy is sufficient to break the dissociative bond immediately. We also suggest how to excite these quasi-coherent vibrations above the dissociation threshold, that is, by means of a series of selective femtosecond IR laser pulses (the pumping process) and how to discover them, namely, by femtosecond UV laser pulses (the probing process). The new type of quasi-coherent vibrations in the continuum of the ground electronic state should be distinguished from other well-known quasi-coherent states or resonances with energies above the dissociation threshold. First, the molecules may be prepared in electronically excited states where they may vibrate quasi-coherently before they eventually dissociate, that is, by tunneling through a potential barrier (predissociation) or by electronic transitions to lower, dissociative electronic states (dissociative internal conversion, IC). These types of quasi-coherent molecular vibrations in electronically excited states have been prepared and monitored since the early days of femtosecond chemistry (see ref 2 and the books and reviews^{3–5}). In contrast, we consider quasi-coherent molecular vibrations in the ground electronic state that do not decay by tunneling through any potential barriers or by electronic transitions. Second, molecules may possess vibrational resonances with energies E_r above the dissociation thresholds and with finite lifetimes τ_r , both in the electronic ground and excited states. In ideal cases of isolated, that is, nonoverlapping, resonances, they give rise to corre-

sponding peaks in the dissociative absorption spectra, with specific energies E_r and widths Γ_r such that

$$\tau_r \Gamma_r \approx \hbar \quad (1)$$

Beautiful examples of experimental spectra indicating vibrational resonances in the electronic ground and excited states are summarized in ref 6 and in the survey,⁷ together with theoretical simulations, respectively. On the theoretical side, these vibrational resonances are described by representative molecular wave packets Ψ_r with corresponding (approximate) exponential decay of the autocorrelation function

$$\langle \Psi_r(0) | \Psi_r(t) \rangle = e^{-iEt/\hbar} \quad (2)$$

where

$$E = E_r - i\Gamma_r/2 \quad (3)$$

corresponding to a Lorentzian spectral peak at energy E_r and with width Γ_r .⁸ In contrast, the autocorrelation function of the present quasi-coherent vibrations are entirely nonexponential (see below). Third, the vibrational resonances 1–3 correspond to classical periodic orbits, embedded in the continuum, for a recent survey (see ref 9). By definition, these orbits are periodic; that is, they must not decay, and this is again in contrast with the present quasi-coherent vibrations, which are represented by molecular wave packets $\Psi(t)$, which will eventually dissociate, even though with a rather long decay time ($\gg 10$ ps). The present model excitation of quasi-coherent vibrations in the continuum by means of a series of selective IR laser pulses provides an extension of previous work on IR laser-pulse excitations of vibrational eigenstates,^{10–12} zero-order states,¹³ and even dissociation.¹⁴ Excitations of bound coherent vibrations, that is, with energies below the dissociation threshold, by means of IR laser pulses have been published in refs 15 and 16, even in combination with subsequent UV photodissociations for selective bond breaking. The use of IR pump plus UV probe laser pulses for preparations and monitoring of excited vibrational eigenstates has been documented in ref 17. For reviews, see refs 18 and 19. The present quasi-coherent vibrations in the continuum of the ground electronic state are discovered by means of molecular wave-packet simulations. For simplicity,

† Permanent address: National Academy of Sciences of Belarus, B. I. Stepanov Institute of Physics, Skaryna ave. 70, 220602 Minsk, Republic of Belarus.

we use a two-dimensional model representing a molecule in the electronic ground state S_0 , with dissociative bond a and nondissociative “spectator” bond b . The existence of (at least) two vibrational degrees of freedom (one of them dissociative) will turn out to be essential; that is, the effect is not expected to exist in diatomic molecules. As a specific model system, we consider HONO_2 , where the dissociative bond is $a = r(\text{N}-\text{O})$ and the nondissociative bond $b = r(\text{O}-\text{H})$. The other degrees of freedom are not considered in this paper, since we aim at the demonstration of the effect in principle, but with realistic parameters, ab initio potential-energy surfaces, and dipole functions. We consider HONO_2 as a candidate, but an accurate simulation would require a nine-dimensional wavepacket propagation, which is beyond the scope of the present paper (see the conclusion section and the comments on related experimental work in refs 20–22). The paper is organized as follows. In section 2, we present our model, adapted from ref 23, and the techniques. The results are in section 3 and the discussion and conclusions in section 4.

2. Model and Techniques

The laser-driven molecular dynamics of our model system in the electronic ground (0) and excited (1) states is described by molecular wave functions $\Psi_0(t)$ and $\Psi_1(t)$. These are obtained as solutions of the time-dependent Schrödinger equation

$$i\hbar \frac{\partial}{\partial t} \begin{pmatrix} \Psi_0 \\ \Psi_1 \end{pmatrix} = \begin{pmatrix} H_{00} & H_{01} \\ H_{10} & H_{11} \end{pmatrix} \begin{pmatrix} \Psi_0 \\ \Psi_1 \end{pmatrix} \quad (4)$$

with the Hamilton operator

$$H_{ij} = T\delta_{ij} + V_{ij}\delta_{ij} - \vec{\mu}_{ij}\vec{E}(t) \quad (5)$$

including the kinetic, adiabatic potential, and semiclassical dipole coupling terms. For simplicity, we neglect diabatic, non Born–Oppenheimer type kinetic couplings as well as rotations such that the angles Θ_{ij} between the molecular (transition) dipoles $\vec{\mu}_{ij}$ and the electric field $\vec{E}(t)$ are fixed. For convenience, we shall employ the optimal molecule-field orientation that yields the maximum excitation.²³ Moreover, we use the two-dimensional model where

$$T = p_a^2/(2\mu_a) + p_b^2/(2\mu_b) + p_a p_b \cos(\alpha)/m \quad (6)$$

with contributions for the kinetic energies of the dissociative bond a , the nondissociative bond b , and their kinetic coupling. The corresponding reduced masses are μ_a , μ_b , and m , and α is the bond angle. As a specific example, we consider the case of HONO_2 (adapted from ref 23); that is, we set $a = r(\text{NO})$, $b = r(\text{OH})$, $\mu_a = \mu_{\text{ON}}$, $\mu_b = \mu_{\text{OH}}$, $m = m_{\text{O}}$, and $\alpha = 103.4^\circ$, where N denotes the NO_2 group, which is treated as one particle. The electric field \vec{E} is oriented along the OH bond. The relevant adiabatic potentials V_{ij} are obtained from quantum-chemical CASSCF^{24,25} ab initio calculations using the Dunning²⁶ triple- ζ basis set, which has been augmented by a set of 5d and 7f polarization functions on the heavy atoms as well as by 3p and 5d polarization functions on the hydrogen atom. All calculations have been done with the MOLPRO96 package of ab initio programs.²⁷ The ab initio calculations also yield the dipole functions $\vec{\mu}_{00}$ and $\vec{\mu}_{01} = \vec{\mu}_{10}$ ($\vec{\mu}_{11}$ is not used in the present simulations).

The electric field is modeled as a series of linearly polarized laser pulses with amplitudes E_i , frequencies ω_i , \sin^2 shapes, and pulse durations from t_i to $t_i + t_{pi}$; that is, it has the nonvanishing

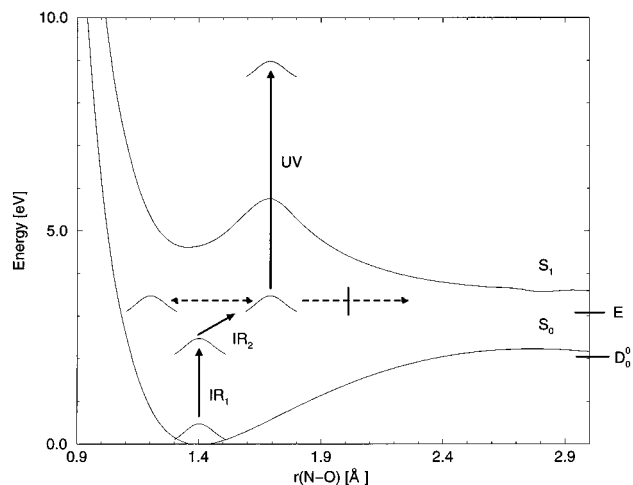


Figure 1. Pump–probe spectroscopy of quasi-coherent molecular vibrations in the electronic ground state with energy E above the dissociation threshold D_0^0 . The vibrations are prepared by two infrared laser pulses $\text{IR}_1 + \text{IR}_2$ and monitored by the UV laser pulse (continuous arrows). The general scheme is illustrated for the two-dimensional model system including the dissociative bond $a = r(\text{N}-\text{O})$ and the nondissociative spectator bond $b = r(\text{O}-\text{H})$ of HONO_2 . The figure shows the quantum-chemical ab initio potential-energy surface for the ground and excited electronic states S_0 and S_1 along bond a , together with schematic snapshots of the laser-driven molecular wave packet and its quasi-coherent vibration between outer and inner turning points (dashed arrows), without any significant dissociations (broken dashed arrow) on the picosecond time scale.

component

$$E(t) = \sum_i E_i(t) \cos[\omega_i(t - t_i)] \times \sin^2[\pi(t - t_i)/t_{pi}] \Theta(t - t_i) \Theta(t_i + t_{pi} - t) \quad (7)$$

Initially, the molecule is assumed to be in its ground vibrational and ground electronic state.

$$\begin{pmatrix} \Psi_0(t=0) \\ \Psi_1(t=0) \end{pmatrix} = \begin{pmatrix} \Phi_{0,00} \\ 0 \end{pmatrix} \quad (8)$$

In general, the vibrational eigenstates Φ_{0,v_a,v_b} are evaluated by means of the Fourier grid method,²⁸ and they are labeled by the dominant number of vibrational quanta v_a and v_b in bonds a and b , respectively. The time evolution of the molecular wave packet driven by the laser field is then evaluated by means of standard propagation techniques.²⁹

3. Results

The strategy toward the preparation and monitoring of the new type of highly excited quasi-coherent molecular vibrations by means of ultrashort laser pulses is indicated in Figure 1. First, an IR laser pulse (denoted IR_1 in Figure 1) excites the nondissociative “spectator bond” b to a highly excited vibrational state, close to a molecular eigenstate with $v_b > 0$ quanta in bond b but 0 quanta in the dissociative bond a . In the present case, the IR_1 laser parameters $E_1 = 174.32$ MV/cm, $\omega_1 = 3289.28$ cm^{-1} , $t_1 = 0$ fs, and $t_{p1} = 500$ fs yield $\Psi_0(t = t_{p1}) \approx \Phi_{0,v_a=0,v_b=4}$, since $\hbar\omega$ is tuned to the corresponding energy gap, $4\hbar\omega_1 \approx E_{0,04} - E_{0,00}$. Second, the next IR laser pulse (denoted IR_2 in Figure 1) excites the dissociative bond a by driving the wave packet quasi-coherently toward longer bond lengths a . In the present case, the laser parameters $E_2 = 137.29$ MV/cm, $\omega_2 = 714.77$ cm^{-1} , $t_2 = t_{p1}$ (i.e., the second pulse IR_2 starts

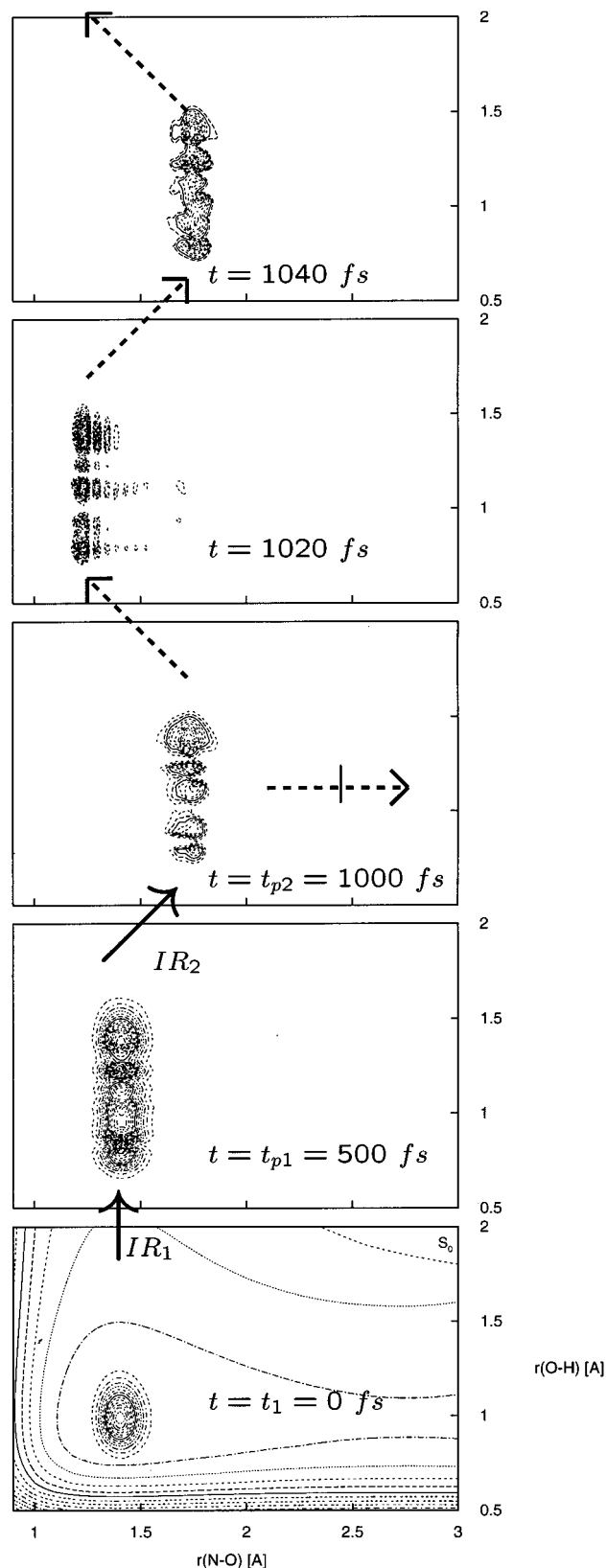


Figure 2. Quasi-coherent vibration (dashed arrows) of the two-dimensional model system representing the dissociative and nondissociative bonds $a = r(\text{N}-\text{O})$ and $b = r(\text{O}-\text{H})$ of HONO_2 in the ground electronic state, and its preparation by two infrared laser pulses $\text{IR}_1 + \text{IR}_2$ (continuous arrows). The snapshots of the molecular wave packet correspond to those shown in Figure 1, but here, they are represented by two-dimensional equidensity contours superimposed on ab initio equidensity contours for the ground electronic state S_0 .

immediately after the first one IR_1 , and $t_{p2} = 500$ fs yield the wave packet $\Psi_0(t = t_{p1} + t_{p2})$. It still contains approximately

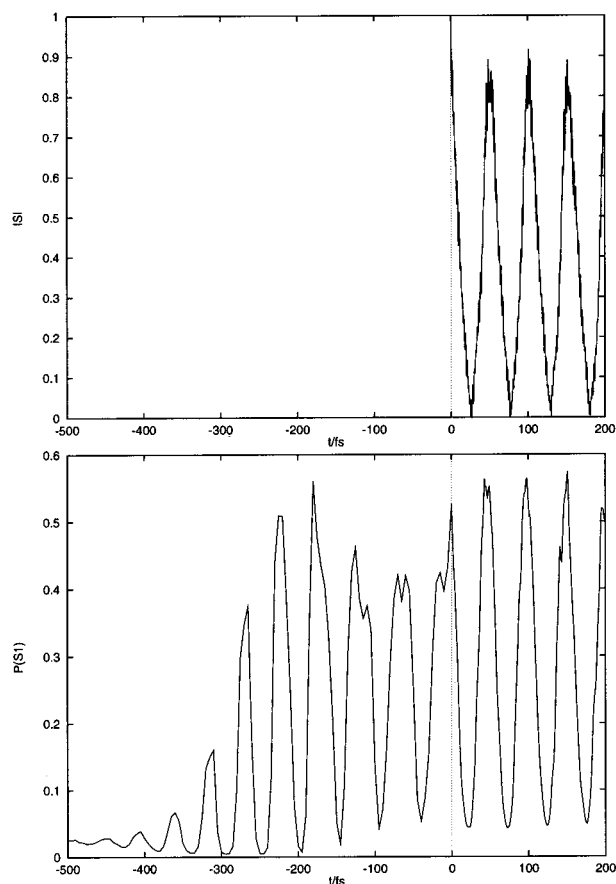


Figure 3. Quasi-coherent vibration of the two-dimensional wave packet $\Psi_0(t)$ with energy E above the dissociation threshold D_0^0 of the ground electronic state, manifested by the autocorrelation function $S_0(t) = \langle \Psi_0(t_{p1} + t_{p2}) | \Psi_0(t) \rangle$ (top) and the $\text{IR}_1 + \text{IR}_2 + \text{UV}$ pump-probe spectrum (bottom), which shows the population $P(S_1)$ of the electronic excited state after the probe pulse as a function of the time delay between the pump and probe laser pulses $\tau = t - t_{p1} - t_{p2}$, which is measured from the end of the preparation process, i.e., after the two $\text{IR}_1 + \text{IR}_2$ laser pulses (cf. Figures 1 and 2). The signal for negative delay times τ monitors the “creation” of the quasi-coherent vibration.

$\nu_b = 4$ quanta in bond b , but now it is transferred to the rather large value of bond $a = a^\ddagger$, which, incidentally, corresponds to the transition-state configuration “ \ddagger ” of the potential energy surface V_{11} of the electronic excited state. The appearance (and, as we shall see, subsequent recurrences) of the wave packet $\Psi_0(t = t_{p1} + t_{p2})$ at “ \ddagger ” is monitored by the third laser pulse (indicated as UV in Figure 1), with UV frequency $\omega_3 = 44360 \text{ cm}^{-1}$, which proved to be the optimal choice for efficient monitoring. The other parameters of the UV probe laser pulse have been chosen as $E_3 = 130 \text{ GV/m}$, $t_{p3} = 10$ fs, with a delay time $\tau = t_3 - (t_{p1} + t_{p2})$ between the UV probe and the two IR_1 and IR_2 pump laser pulses, which is varied from -500 to 200 fs.

The total energy, which has been absorbed by the molecule from the two $\text{IR}_1 + \text{IR}_2$ laser pulses is approximately $E_{\text{IR}_1 + \text{IR}_2} \approx 4\hbar\omega_1 + 15\hbar\omega_2 = 3.0 \text{ eV}$ and is well above the ON bond energy, $D_0^0 = 2.14 \text{ eV}$. In fact, it is also larger than the small potential barrier $V_{\text{barr}} = 2.20 \text{ eV}$ of the potential energy surface V_{00} in the electronic ground state (see Figure 1). Note that the energy of the wave packet after the first pulse IR_1 is $E_{\text{IR}_1} = 2.08 \text{ eV} < D_0^0$; that is, this wave packet still belongs to the bound states. By intuition, the value of $E_{\text{IR}_1 + \text{IR}_2} > D_0^0$ would suggest that the highly excited wave packet $\Psi_0(t_{p1} + t_{p2})$, which has been prepared by the pump laser pulses $\text{IR}_1 + \text{IR}_2$, should dissociate immediately. To test this working hypothesis, we

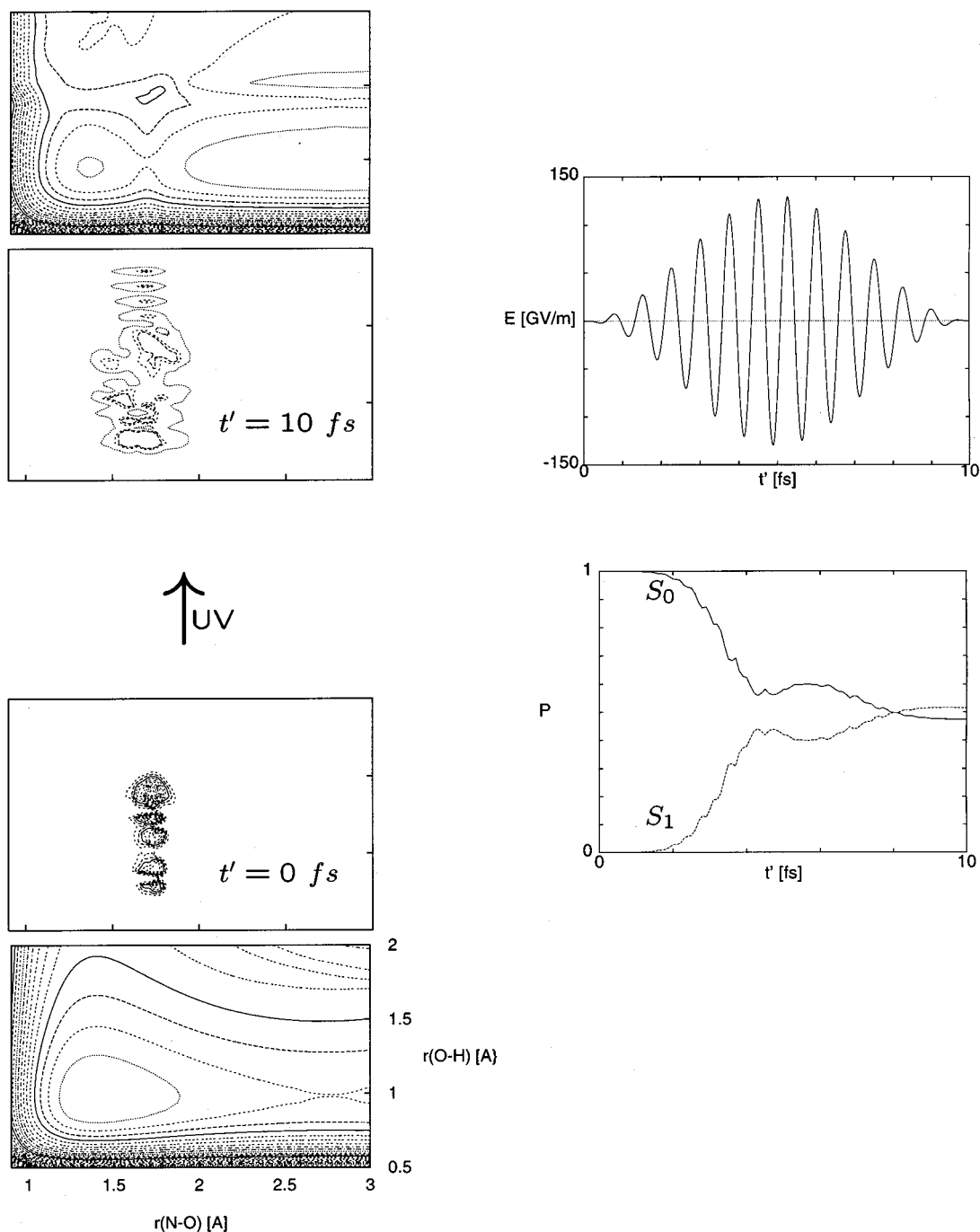


Figure 4. Details of the quasi-coherent vibrations of the wave packet $\Psi_0(t)$ within the two-dimensional model (cf. Figures 1–3). The left and bottom panel shows the wave packet Ψ_0 after its preparation by the $\text{IR}_1 + \text{IR}_2$ laser pulses, i.e., $t' = t - t_{p1} - t_{p2} = 0$, superimposed on the potential-energy surface of the electronic ground state. The top left panel shows the wave packet $\Psi_1(t)$, which has been created on the potential-energy surface of the state S_1 at the end of the UV probe pulse. The UV pulse and the resulting populations P_0 and P_1 of the ground and excited electronic states are shown in the right panels.

have continued the propagation of $\Psi(t)$ beyond times $t > t_{p1} + t_{p2}$ and found a fascinating result: instead of dissociation, the wave packet starts to move toward shorter bond length a followed by quasi-coherent vibrations along this bond. This is indicated schematically in Figure 1 and more quantitatively in Figure 2, which documents the preparation of the wave packet

$$\Psi_0(t=0) = \Phi_{0,00} \xrightarrow{\text{IR}_1} \Psi_0(t=t_{p1}) \approx \Phi_{0,04} \xrightarrow{\text{IR}_2} \Psi_0(t+t_{p1}+t_{p2}) \quad (9)$$

as well as the subsequent quasi-coherent vibration of Ψ_0 ,

essentially between outer and inner turning points at long and short bond lengths of a and with vibrational period $\tau \approx 40$ fs. Another documentation of this new type of quasi-coherent vibrations, that is, with energy $E > D_0^0$, is the autocorrelation function

$$S_0(t) = \langle \Psi_0(t_{p1} + t_{p2}) | \Psi_0(t) \rangle \quad (10)$$

which is shown in the Figure 3 (top). Apparently, $|S_0(t)|$ oscillates between large (~ 1) and small (~ 0) values in a quasi-periodic fashion, due to the quasi-coherent vibrations that cause the recurrences of $\Psi_0(t)$ at its original configuration $\Psi_0(t_{p1} +$

t_{p2}) at the outer turning point “ \ddagger ”. In Figure 1 we also suggest how these recurrences can be monitored by $\text{IR}_1 + \text{IR}_2 + \text{UV}$ pump–probe spectroscopy. The resulting signal is shown in Figure 3 (bottom). Obviously, it is similar to the autocorrelation function $S_0(t)$, shown in Figure 3 (top), thus reflecting the signature of the quasi-coherent vibrations. In addition, this signal monitors the “creation” of the quasi-coherent vibration during the negative delay time τ , where the UV probe pulse is switched on when the second pulse IR_2 is still active. Figure 4 documents the probing of $\Psi_0(t)$ at “ \ddagger ” in more detail; that is, the UV probe pulse transfers part of $\Psi_0(t)$ from the potential-energy surface of the ground electronic state to $\Psi_1(t)$ in the excited state in a Franck–Condon-type, nearly vertical transition. Since $\Psi_1(t)$ is actually created at the potential barrier “ \ddagger ” of V_{11} , this gives rise to rich subsequent nuclear wave-packet dynamics; that is, $\Psi_1(t)$ separates into two fragments that dissociate either directly or indirectly, that is, after certain vibrations within and subsequent tunneling processes out of the local well of V_{11} (see Figure 1). Ultimately, the entire wave packet $\Psi_1(t)$ will dissociate, and both the $S_0 \rightarrow S_1$ absorption intensities and the yield of rapid³⁰ products (e.g., to $\text{OH} + \text{NO}_2$) could serve as experimental measures for the norm of $\Psi(t)$, which monitors the quasi-coherent recurrences of $\Psi_0(t)$ at “ \ddagger ”.

4. Discussion

The present discovery of quasi-coherent molecular vibrations with energies well above the dissociation threshold in the ground electronic state of a two-dimensional model system, based on ab initio potential-energy surfaces and (transition) dipole functions of HONO_2 , calls for several extensions. First, it is a challenge to verify the effect in more realistic models that treat the respective molecules in more or full dimensionality. One may anticipate that the quasi-coherent molecular vibrations will then have to compete against dissipative processes, in particular intramolecular vibrational redistribution (IVR), and this should cause some overall spreading of the molecular wave packet such that the nearly ideal recurrences documented in Figures 2 and 3 will tend to be washed out to some extent. Similar effects of decreasing recurrences upon increasing dimensionality have been observed, for example, for quasi-coherent vibrations in electronically excited states, owing to conical intersections of several potential energy surfaces.³¹ In the present case, however, we are dealing with molecular dynamics exclusively in the electronic ground state, and here, the quasi-coherent vibrations might be more robust, since the pathways to dissipative dynamics are more restricted than in electronically excited states. Ultimately, the “survival” of the quasi-coherent vibrations should depend on the intramolecular coupling in the electronic ground state and the related time scales for IVR. This calls for systematic investigations of the favorable conditions for observing the effect in real systems. Second, it is a challenge to discover the effect experimentally. The choice of an ideal system should, of course, depend on the results of the above-mentioned systematic investigations. Meanwhile, we suggest that our model system, HONO_2 , should be considered as a candidate. Our suggestion is based on the rather favorable comparison of the theoretical result for the period of the quasi-coherent vibration, $\tau \approx 40$ fs, and the recent experimental result for IVR, that is, $\tau_{\text{IVR}} \approx 12$ ps,²² albeit in the domain of lower excitations. At higher energies, such as in the present case of quasi-coherent vibrations above the dissociation threshold, the value of τ_{IVR} may decrease, but previous experimental demonstrations of IR + UV mediated chemistry^{20,21} imply that τ_{IVR} should still be sufficiently long, $\tau_{\text{IVR}} > 40$ fs. As a consequence,

the quasi-coherent vibration may survive at least for several oscillations, and this should show up in pump–probe spectra similar to that of the pure, two-dimensional reference shown in Figure 3 except for some damping due to IVR. Third, the systematic theoretical investigations should also yield the molecular mechanism that allows the phenomenon of quasi-coherent vibrations above the dissociation threshold. Apparently, the molecule has enough energy for dissociation. But part of it is not available, since it is stored in the nondissociative “spectator” mode. Our model accounts for all the kinetic and potential couplings of the two bonds a and b , but these couplings turn out to be so weak that it takes a very long time ($\tau \gg 10$ ps) before the energy can flow from the spectator b to the dissociative bond a . Similar weak couplings are also responsible for rather long lifetimes of vibrational resonances in other model systems.³² By analogy, we consider experimental observation of similar resonances⁶ by means of CW lasers as encouraging; that is, it should likewise be possible to prepare and observe the quasi-coherent vibrations with energy well above the dissociation threshold by means of ultrashort laser pulses, which can compete against IVR.

Acknowledgment. We thank Dr. M. Gutmann (Köln) for discussions. Financial support by the Deutsche Forschungsgemeinschaft (Project Ma 515/15-1) and by the Fond der chemischen Industrie (to J.M.) is also gratefully acknowledged. The computations have been carried out on our HP 9000/S 750 workstations and on the SGI Origin2000 of the Computing Center (ZEDAT) of the FU Berlin.

References and Notes

- (1) Schrödinger, E., *Naturwissenschaften* **1926**, *14*, 666.
- (2) Rose, T. S.; Rosker, M. J.; Zewail, A. H. *J. Chem. Phys.* **1988**, *88*, 6627.
- (3) Manz, J., Wöste, L., Eds. *Femtosecond Chemistry*; VCH Verlagsgesellschaft: Weinheim, 1995; Vols. 1 and 2.
- (4) Zewail, A. H. *J. Phys. Chem.* **1996**, *100*, 12701.
- (5) Manz, J. In *Femtochemistry and Femtobiology*; Sundström, V., Ed.; World Scientific: Singapore, in press.
- (6) Neumark, D. M. *Acc. Chem. Res.* **1992**, *26*, 33.
- (7) Huber, J. R.; Schinke, R. *J. Phys. Chem.* **1993**, *97*, 3463.
- (8) Bisseling, R. H.; Kosloff, R.; Manz, J.; Mrugala, F.; Römlert, J.; Weichselbaumer, G. *J. Chem. Phys.* **1987**, *86*, 2626.
- (9) Gaspard, P.; Burghardt, I. *Adv. Chem. Phys.* **1997**, *101*, 491.
- (10) Paramonov, G. K.; Savva, V. A. *Phys. Lett. A* **1983**, *97*, 340.
- (11) Gabriel, W.; Rosmus, P. *J. Phys. Chem.* **1993**, *97*, 12644.
- (12) Liu, L.; Muckerman, J. T. *J. Chem. Phys.* **1997**, *107*, 3402.
- (13) Paramonov, G. K. *Chem. Phys. Lett.* **1996**, *250*, 505.
- (14) Korolkov, M. V.; Paramonov, G. K.; Schmidt, B. *J. Chem. Phys.* **1996**, *105*, 10874.
- (15) Henriksen, H. E. *Adv. Chem. Phys.* **1995**, *91*, 433. Armstrup, B.; Henriksen, N. E. *J. Chem. Phys.* **1992**, *97*, 8285.
- (16) Shapiro, M.; Brumer, P. *J. Chem. Phys.* **1993**, *98*, 201.
- (17) Dohle, M.; Manz, J.; Paramonov, G. K.; Quast, H. *Chem. Phys.* **1995**, *197*, 91.
- (18) Paramonov, G. K. In *Femtosecond Chemistry*; Manz, J., Wöste, L., Eds.; VCH Verlagsgesellschaft: Weinheim, 1995; Vol. 2, pp 671–712.
- (19) Korolkov, M. V.; Manz, J.; Paramonov, G. K. *Adv. Chem. Phys.* **1997**, *101*, 327.
- (20) Sinha, A.; Vander Wal, R. J.; Butler, L. J.; Crim, F. F. *J. Phys. Chem.* **1987**, *91*, 4645.
- (21) Sinha, A.; Vander Wal, R. J.; Crim, F. F. *J. Chem. Phys.* **1990**, *92*, 401.
- (22) Bingemann, D.; Gorman, M. P.; King, A. M.; Crim, F. F. *J. Chem. Phys.* **1997**, *107*, 661.
- (23) Oppel, M.; Paramonov, G. K. *Chem. Phys.*, in press.
- (24) Werner, H.-J.; Knowles, P. J. *J. Chem. Phys.* **1985**, *82*, 5053.
- (25) Knowles, P. J.; Werner, H.-J. *Chem. Phys. Lett.* **1985**, *115*, 259.
- (26) Dunning, T. H., Jr. *J. Chem. Phys.* **1971**, *55*, 716.
- (27) MOLPRO is a package of ab initio programs written by H.-J. Werner and P. J. Knowles, with contributions from J. Almlöf, R. D. Amos, A. Berning, M. J. O. Deegan, F. Eckert, S. T. Elbert, C. Hampel, R. Lindh,

W. Meyer, A. Nicklass, K. Peterson, R. Pitzer, A. J. Stone, P. R. Taylor, M. E. Mura, P. Pulay, M. Schuetz, H. Stoll, T. Thorsteinsson, and D. L. Cooper.

(28) Marston, C. C.; Balint-Kurti, G. G. *J. Chem. Phys.* **1989**, *91*, 3571.

(29) Feit, M. D.; Fleck, J. A. *J. Comput. Phys.* **1982**, *47*, 412. Feit, M. D.; Fleck, J. A. *J. Chem. Phys.* **1982**, *78*, 301. Feit, M. D.; Fleck, J. A. *J. Chem. Phys.*, **1984**, *80*, 2578.

(30) August, J.; Brouard, M.; Simons, J. P. *J. Chem. Soc., Faraday Trans. 2*, **1988**, *84*, 587.

(31) Domcke, W.; Stock, G. *Adv. Chem. Phys.* **1997**, *100*, 1. Köppel, H.; Cederbaum, L. S.; Domcke, W.; Shaik, S. S. *Angew. Chem., Int. Ed. Engl.* **1983**, *22*, 210.

(32) Hartke, B.; Manz, J.; Mathis, J. *Chem. Phys.* **1989**, *93*, 123.